

The Use of High-Pressure Nuclear Magnetic Resonance to Study Protein Folding

Michael W. Lassalle and Kazuyuki Akasaka

Summary

Recent development of high-pressure cells for a variety of spectroscopic methods has enabled the use of pressure as one of the commonly used perturbations along with temperature and chemical perturbations to study folding/unfolding reactions of proteins. Although various high-pressure spectroscopy techniques have their own significance, high-pressure nuclear magnetic resonance (NMR) is unique in that it allows one to gain residue-specific and atom-detailed information from proteins under pressure. Furthermore, because of a peculiar volume property of a protein, high-pressure NMR allows one to obtain structural information of a protein in a wide conformational space from the bottom to the upper region of the folding funnel, giving structural reality for the “open” state of a protein proposed from hydrogen exchange. The method allows a link between equilibrium folding intermediates and the kinetic intermediates, and manifests a new view of proteins as dynamic entities amply fluctuating among the folded, intermediate, and unfolded sub ensembles. This chapter briefly summarizes the technique, the principle, and the ways to use high-pressure NMR for studying protein folding.

Key Words: Pressure; protein folding; thermodynamic stability; volume change; structures of folding intermediates; high-pressure NMR; pressure-jump.

1. Introduction

Pressure perturbation is increasingly important in studies of protein folding, stability, conformational flexibility, and aggregation. A keyword search on HighWire and Medline with keywords: high pressure-protein-nuclear magnetic resonance (NMR) shows that there has been a dramatic increase in the number of pressure-related studies of proteins (**Fig. 1**). The dramatic increase is assisted by technical developments for high-pressure studies in a variety of spectroscopic measurements at high pressure including X-ray scattering (**1,2**), fluorescence (**3–6**), Fourier-transform infrared spectroscopy (**6–10**) and ultraviolet-visible derivative spectroscopy

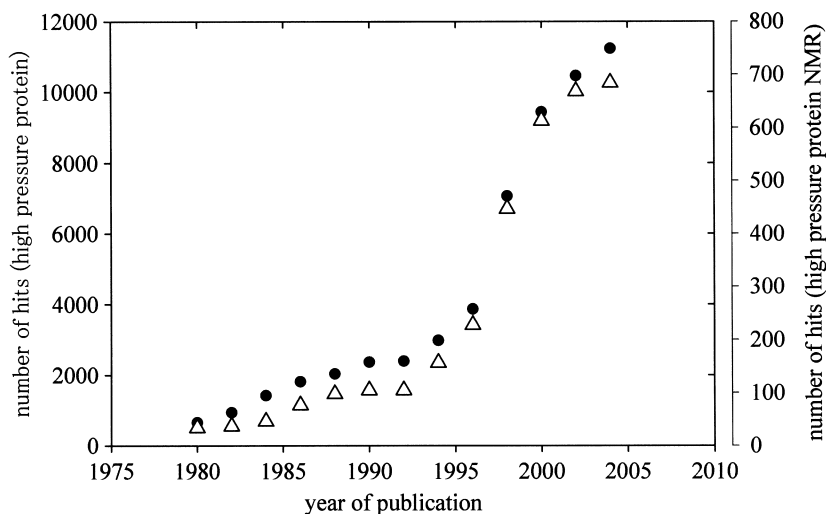


Fig. 1. Keyword search in HighWire and Medline as function of publication year. Circles: key words utilized: high pressure-protein. Triangle: key words utilized: high pressure-protein-nuclear magnetic resonance.

(11), kinetic processes under pressure (12,13), and pressure-jump techniques (14–16). In particular, the recent advancement in high-pressure NMR techniques has renewed interest in high-pressure studies of proteins, it allows to gain residue-specific or atom-detailed information from proteins under pressure.

2. Materials

Buffers to be used for pressure studies are preferred to have little variation of pKa with pressure. There is no complete buffer in this sense, but the following buffers are relatively inert to pressure variation. One must be aware, however, that those buffers inert to pressure variation tend to be more susceptible to temperature variation. Useful buffers are maleic acid ($\Delta V^\circ = -5.1 \text{ cm}^3 \text{ mol}^{-1}$), MES ($\Delta V^\circ = 3.9 \text{ cm}^3 \text{ mol}^{-1}$), Tris ($\Delta V^\circ = 4.3 \text{ cm}^3 \text{ mol}^{-1}$), or imidazole buffers ($\Delta V^\circ = 1.8 \text{ cm}^3 \text{ mol}^{-1}$) (17). As chemical shift standard, the singlet signal of DSS is to be set at origin ($\delta = 0$). However, this often overlaps with some methyl proton signals in the ^1H NMR spectrum. The authors found that dioxane can be used as a convenient secondary standard, as it gives a sharp singlet at $\delta = 3.75$ ppm downfield from DSS nearly independently of pressure.

3. Methods

3.1. High-Pressure NMR Techniques

Recent contributions to high-pressure NMR study of proteins are mainly attributable to the groups of Jonas (18) and Akasaka (19), in addition to those



Fig. 2. A pressure-resisting quartz cell and the protecting Teflon capsule used for the on-line cell high-pressure nuclear magnetic resonance system.

of Kalbitzer (20), Wand (21), and Markley (22). The heart in designing high-pressure NMR techniques is how to design a pressure-resistant cell in a small signal detection space by maintaining the highest possible homogeneity in both static and radiofrequency magnetic fields without losing sensitivity of detection. Typically two cell designs have been utilized. The former group (18) preferred an autoclave design, which has the advantage of larger sample volume and high attainable pressure (~ 900 MPa). Here, receiver coils must be self-designed within the autoclave. The cell contains sufficient volume and applies very well to recording one-dimensional (1D) ^1H NMR spectra of proteins. A major problem lies in the difficulty to obtain well-resolved two- or multidimensional spectra where multiple nuclei must be simultaneously excited within a highly homogeneous static and radiofrequency magnetic fields spanning the entire sample space. The latter group (19) developed pressure-resisting cells (Fig. 2) made up initially of glass, then of quartz (both hand-made) (23), and used them on a commercial NMR probe. This is the on-line cell high-pressure NMR system described in some detail in the following section. Although the inner space of the pressure-resistive cell is so small (typically ~ 20 μL ; Fig. 2) that the signal intensity is inherently low, the field homogeneity can be extremely good and allows all two- or multidimensional spectral measurements, giving

excellent high resolution multidimensional spectra as those obtained with normal 5-mm tubes at 1 bar. Therefore, the on-line cell high-pressure method has a higher versatility than the autoclave method for protein studies. Some efforts have been made to increase the sample volume by utilizing sapphire cells with limited success (20,21).

The maximum pressure range of the quartz cell method is normally limited from 200 to approx 400 MPa (because cells break at higher pressure), this relatively mild pressure range has been sufficient in many proteins to a variety of studies including folding intermediates (24), conformational dynamics (25), local disordering (26), kinetic intermediates (27), stability (28), energy-landscapes (29), and dissociation/association of proteins (30). Although many proteins may not fully unfold below approx 400 MPa, 100% unfolding is actually not required in high-pressure NMR measurements because the onset of full unfolding is recognized if all the cross peaks begin to lose their intensities, say up to approx 20%, in a concerted manner in a typical well-resolved two-dimensional (2D) NMR spectra. The applicability of variable-pressure NMR to studies of folding intermediates is also assured by recognizing the general tendency for the decreasing order of tertiary structure as pressure is increased (31). In this chapter, we will concentrate our effort solely to highlight the advantages of high-pressure NMR in the study of thermodynamic stability and folding, but the concept and the method of analysis are applicable to results of any high-pressure spectroscopic measurements.

3.1.1. The On-Line Cell High-Pressure NMR System

The heart of the success of the on-line cell high-pressure NMR method relies on the preparation of pressure-resistive sample cells (23) (Fig. 2). As mentioned, the starting material generally used is transparent quartz capsules or quartz capsules made by synthetic silica. First a perfect clean surface must be obtained; we achieved this goal by etching the glass inside and outside with a dilute hydrofluoric acid solution and by removing micro cracks with fire polishing. Then the quartz capsules are opened at scratched points, and the ends are heated to make a long tail (o.d. = 0.3–1 mm; length = 400–700 mm), a short sealed tail (o.d. = 0.1–0.5 mm; length = 1–2 mm), and a cell body. The short sealed tail enables a bottom design with a small tensile force in a small area. Finally, pyroxylin coating of the short tail, cell body, and long tail is performed. Our final cell has an inside diameter about 0.8–1.0 mm and an outside diameter of 3.0–3.7 mm.

The high-pressure cell assembly consists of a hand oil-pump, a pressure intensifier, and a Heise-Bourdon gage. A 6 m-long SUS-316 high-pressure tube (o.d./ i.d. = 3.0/0.6 mm) transmits the pressure to the top of the high-pressure cell-separator assembly. This assembly consists of a polytetrafluoroethylene (PTFE) safety jacket and the NMR tube described above with a long flexible tail that was bonded to an SUS-316 nozzle with a thermo hard-

ening epoxy adhesive (Araldite AT1). The nozzle is connected through a PTFE connector tube to a PTFE inner tube, which is embedded in a BeCu separator cylinder. Within the PTFE inner tube, two PTFE pistons with a length of 3–4 mm and with diameter about 0.05 mm smaller than the i.d. of the PTFE inner tube are seated. The space between upper and lower pistons is filled with perfluoro-polyether, as it is insoluble in both organic solvent and water and acts as separator between the pressure transmitting system and the NMR sample. An 80:20 mixture of motor oil and kerosene is used as pressure transmitting fluid. Both the NMR tube with flexible long tail and the PTFE inner tube up to the lower PTFE piston are filled with the sample solution, whereas the high-pressure tube up to the upper piston contains the pressure transmitting fluid.

3.2. Methods for Determining Thermodynamic Parameters From High-Pressure Experiment

3.2.1. Basic Equations for Two-State Transition

The thermodynamic stability of proteins has been much less explored in the pressure axis than in the temperature or chemical axis. However, if the solution conditions (chemical compositions) are fixed, the conformational stability of a protein $\Delta G = G_{\text{unfolded}} - G_{\text{folded}}$ is a simultaneous function of both temperature and pressure; thus defining a three-dimensional Gibbs free energy surface on the pressure–temperature plane. Several excellent papers (29,32–34) on multi-dimensional energy landscapes have been published.

The basic equations governing the stability of proteins on the p and/or T axes are given in the following:

1. By taking the pressure dependence of ΔG to the first order at constant temperature,

$$\Delta G = \Delta G_{1\text{bar}}^o + p\Delta V^0 \quad (1)$$

and to the second order,

$$\Delta G_p - \Delta G^o = \Delta V^0(p - p_o) - \frac{\Delta\beta}{2}(p - p_o)^2 \quad (1')$$

2. By taking the “exact” expression for temperature dependence of ΔG and the pressure dependence of ΔG to the second order,

$$\begin{aligned} \Delta G = \Delta G^o - \Delta S^o(T - T^o) - \Delta C_p \left[T \left(\ln \frac{T}{T^o} - 1 \right) + T^o \right] \\ + \Delta V^o(p - p^o) - \frac{\Delta\beta}{2}(p - p^o)^2 + \Delta\alpha(p - p^o)(T - T^o) \end{aligned} \quad (2)$$

Performing a Taylor expansion and neglecting higher order terms with respect to temperature, this equation equals the following:

$$G = \Delta G^o - \Delta S^o(T - T^o) - \frac{\Delta C_p}{2T^o}(T - T^o)^2 + \Delta V^o(p - p^o) \quad (2')$$

$$- \frac{\Delta\beta}{2}(p - p^o)^2 + \Delta\alpha(p - p^o)(T - T^o)$$

Utilizing **Eq. 1** implies that the isothermal compressibility change ($\Delta\beta$) can be assumed to be zero or negligibly small. If this is not the case, **Eq. 1'** must be used. Employing **Eq. 2** or **2'** leads to a multidimensional energy landscape under the assumption that in the temperature and pressure ranges under investigation, heat capacity (ΔC_p), thermal expansion coefficient ($\Delta\alpha$), and isothermal compressibility coefficient ($\Delta\beta$) are constant.

3.2.2. Experiment 1: Simultaneous Change of Pressure and Temperature: Elucidation of a Multidimensional Energy Landscape Using **Eq. 2**

Careful measurements of NMR spectra at varying pressure and temperature is particularly suited to determine the p - T energy landscape of proteins. This is because the folding and/or the unfolding fraction can be assessed accurately, as the NMR intensity for a perfect folded protein is intrinsically known for typical well-isolated NMR signals with no overlaps. As a target protein for our study to obtain an energy landscape on the p - T plane, we chose *Staphylococcal* nuclease (**29**), which is known to closely obey the two-state transition between folded (F) and unfolded (U) state (**22,34,35**), a requirement for the straightforward application of previously mentioned equations. 1D ^1H NMR spectra were measured in deuterated 20 mM MES buffer, pH 5.3, as a function of pressure between 3 and 330 MPa at various temperatures (**Fig. 3**). The well-isolated His8 ϵ proton signals were used to obtain conformational equilibrium $K = [\text{U}]/[\text{F}]$, which, by using the relation $\Delta G = -RT\ln K$, allowed us to obtain experimental $\Delta G = G_{\text{unfolded}} - G_{\text{folded}}$ values as a simultaneous function of pressure and temperature. By least-squares-fitting the experimental ΔG values to **Eq. 2**, we determine all the thermodynamic parameters ΔG^o , ΔS^o , ΔV^o , ΔC^o , $\Delta\beta$, and $\Delta\alpha$, giving a three-dimensional energy landscape shown in **Fig. 4**.

The results demonstrate that combined temperature-pressure-dependent studies can help delineate the free energy landscape of proteins on p - T axes and, hence, help elucidate the features and thermodynamic parameters that are essential for the stability of the native conformational state of proteins.

3.2.3. Experiment 2: Pressure Dependence of 1D ^1H NMR: Elucidation of Thermodynamic Stability Using **Eq. 1**

A more general use of high-pressure NMR for determining thermodynamic stability of proteins ΔG^o and the associated volume change ΔV^o comes from the use of **Eq. 1**. Often small proteins exhibit reasonably good two-state unfolding.

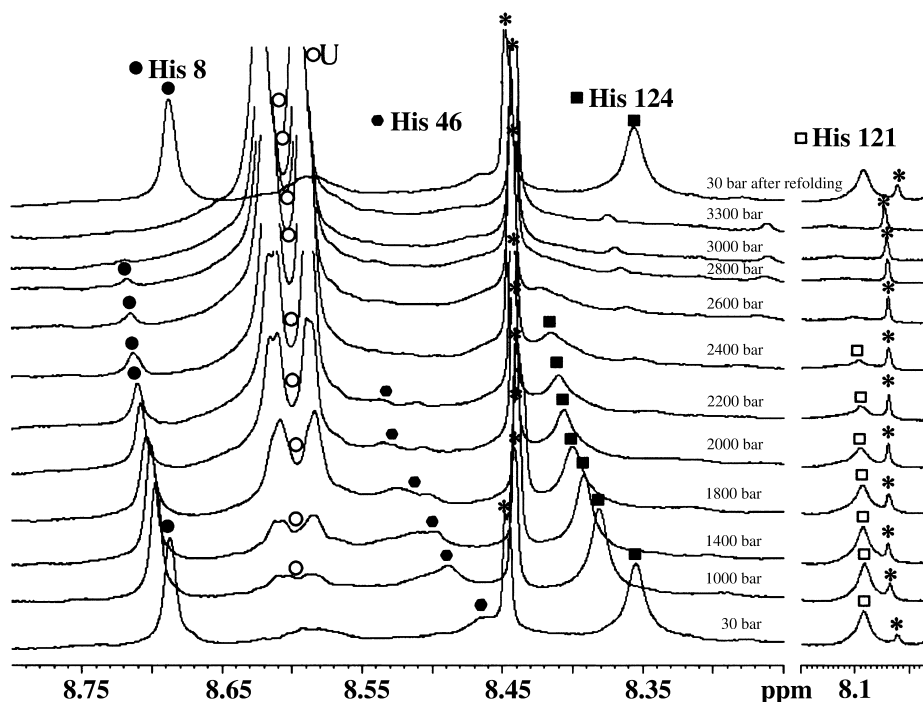


Fig. 3. An example showing the effect of pressure on the one-dimensional ^1H nuclear magnetic resonance spectrum of a globular protein *Staphylococcal* nuclease. * Indicates impurity signals. (Reprinted from ref. 29, with permission from Elsevier.)

In general, pressure effects on folded proteins appear in three major steps (36). Step 1 is a nearly linear compression of the folded conformer. For example, in Fig. 3, the effect of compression on the folded conformer can be seen in the low-field shifts of three His ϵ proton signals. In step 2 a transition takes place from a folded conformer to an alternate conformer with an abrupt change in volume ΔV° . Often, this step is manifested as a decrease of signals from the folded conformer with concomitant increase of new signals from the alternate conformer, in the case of *Staphylococcal* nuclease the unfolded state U. In Fig. 3, this effect is seen in the gradual loss of the native His ϵ proton signals with concomitant appearance of the denatured His ϵ proton signals U as we increase the pressure. Step 3 is a compression of the unfolded conformer U. A linear plot of ΔG against pressure through Eq. 1 gives simultaneously the volume change ΔV° from the slope and the stability at 1 bar ΔG^0 by extrapolation of ΔG to 1 bar. The latter gives an alternative general method to the popular one—determining the stability of a protein structure with guanidium chloride or urea.

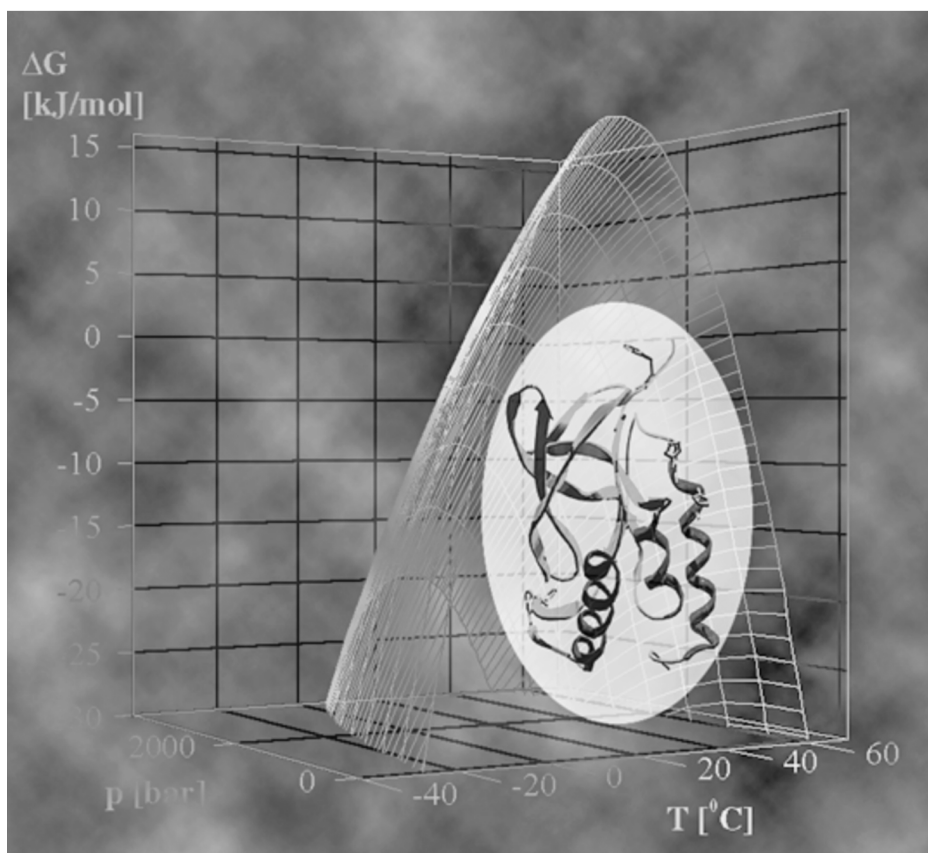


Fig. 4. Three-dimensional free energy landscape of *Staphylococcal* nuclease with its folded structure.

The volume change ΔV^o is an extra parameter we obtain for protein unfolding uniquely from pressure experiment. The origin of the volume change ΔV^o has been discussed in various literatures (37–39) and is considered to originate from the loss of atom defects or cavities within the folded conformer, the hydration of hydrophobic residues upon unfolding and the hydration of charged residues upon unfolding. A consensus is attained such that, all effects combined, the resultant ΔV^o is negative for unfolding of globular proteins under closely physiological conditions (40).

The effect of cavity on the stability ΔG^o and the volume change ΔV^o has been experimentally examined on the wild-type c-Myb R2 sub-domain and its cavity-filling mutant (Fig. 5) using ^1H 1D NMR as a function of pressure (28). The cavity of c-Myb R2 was filled by replacing a Val with a Leu and it was

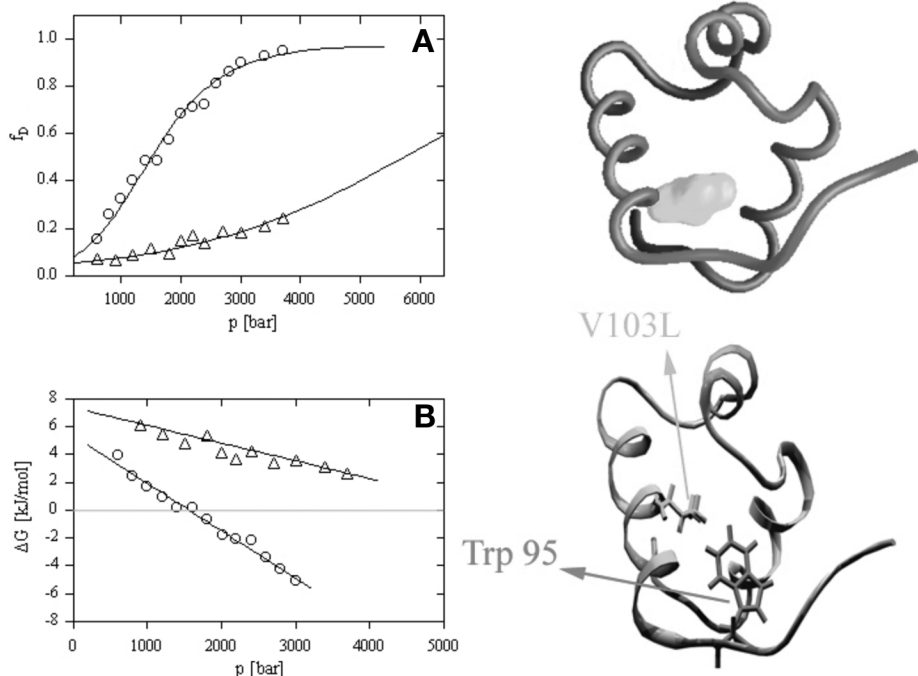


Fig. 5. A cavity-filling mutation leads to a significant loss of ΔV in the c-Myb R2 domain, showing the significant cavity contribution to ΔV . (A) Plot of the unfolded fractions against pressure for the wild-type (○) and the mutant (Δ). (B) Plot of the stability against pressure for the wild-type (○) and the mutant (Δ). Figures on the right shows ribbon models of the wild-type (upper) and the cavity-filling mutant (lower) of the c-Myb R2 domain. (Reproduced with permission from ref. 28.)

confirmed that the tertiary structure is unaltered (41). We obtained ΔG^0 is increased from 5.36 to 7.34 kJ/mol by the cavity-filling mutation, whereas ΔV^0 is changed from -33.9 to -12.6 mL/mol.

Among the three factors that contribute to ΔV^0 , the difference in ΔV_{sol} (hydration term) and ΔV_c (van der Waals volumes of the constitutive atoms) between the two proteins are small enough to be neglected (41) and, therefore, high-pressure unfolding of the native and cavity-filling mutation reveals partial molar volume change (ΔV^0), whereas $\Delta \Delta V^0_{native-mutated}$ reflects the size of the cavity. Comparison of our calculated cavity size 35.3 Å with literature values 33.1 Å (41) shows a good agreement. The decisive effect of cavity on the volume change ΔV has been experimentally verified also in *Staphylococcal* nuclease (38).

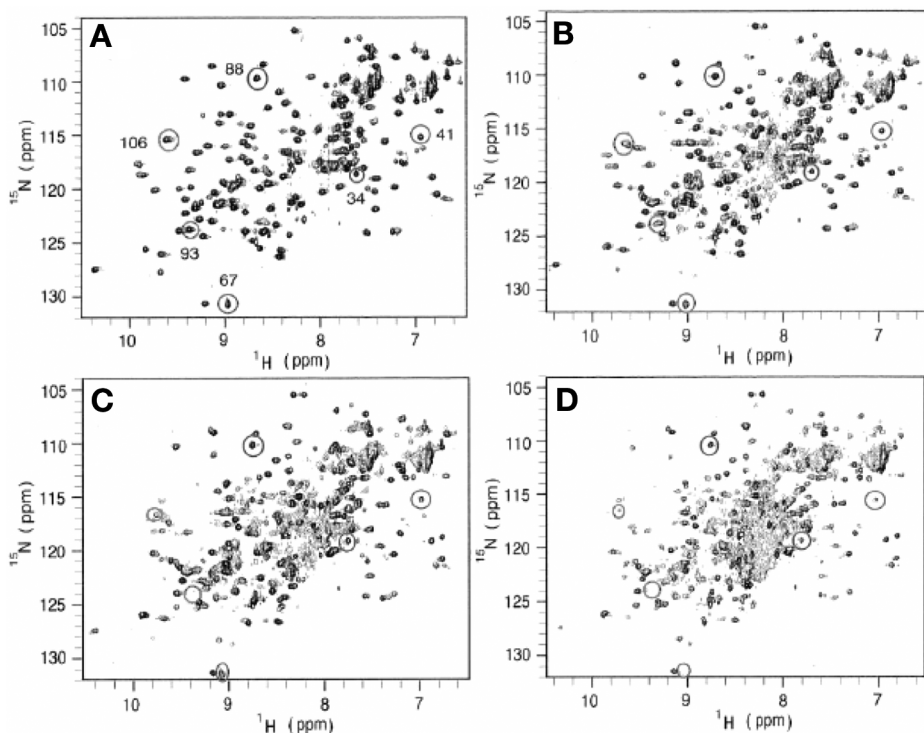


Fig. 6. Two-dimensional $^{15}\text{N}/^1\text{H}$ HSQC spectra of β -lactoglobulin at (A) 3 MPa; (B) 100 MPa; (C) 150 MPa; (D) 200 MPa at pH 2.0 and 36°C, measured at 750 MHz in 95% $^1\text{H}_2\text{O}/5\%$ $^2\text{H}_2\text{O}$. (Reprinted from **ref. 42**, with permission from Elsevier.)

3.2.4. Experiment 3: Pressure Dependence of 2D Heteronuclear NMR (e.g., $^{15}\text{N}/^1\text{H}$ HSQC): Characterization of Folding Intermediates

Detection of intermediates is often considered to be a key to understanding protein-folding process. These cannot be, in general, detected easily in ^1H NMR spectra even under variable pressure. We have to proceed to utilize NMR spectra for residue-specific structural information, which is possible by performing heteronuclear 2D NMR spectra such as ^{15}N - ^1H HSQC as a function of pressure. By comparing molar volume changes (ΔV°) and Gibbs free energy changes (ΔG°) for individual amino acid sites based on **Eq. 1**, we can easily differentiate between an overall cooperative unfolding from local unfolding. By grouping residues having similar ΔG° and ΔV° values together, structural and thermodynamic information can be obtained about locally unfolded or intermediate conformers of the protein (27,42).

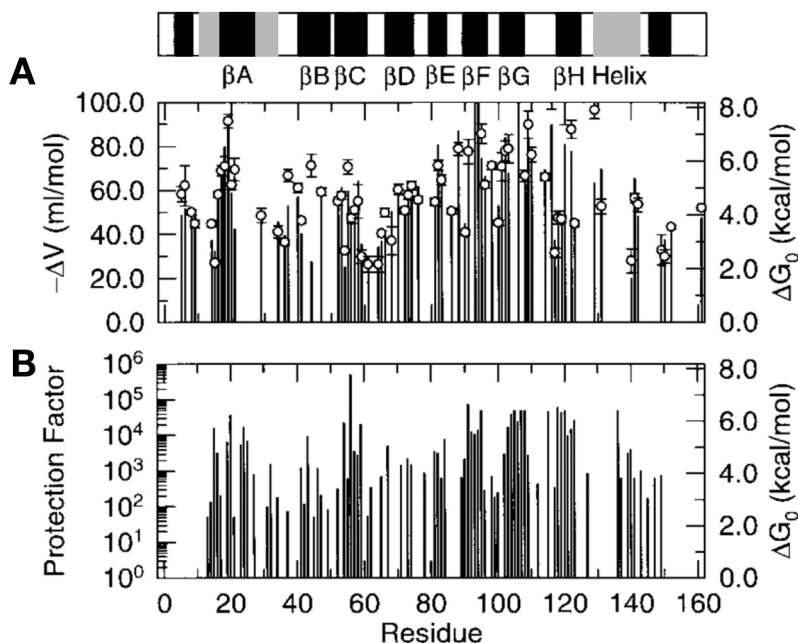


Fig. 7. Plots of (A) ΔG^0 (–) and ΔV (O) determined from high-pressure nuclear magnetic resonance and (B) the protection factor from $^1\text{H}/^2\text{H}$ exchange, for individual residues of β -lactoglobulin. (Reprinted from **ref. 42**, with permission from Elsevier.)

β -Lactoglobulin has a β -barrel structure, inside of which small hydrophobic molecules are bound for transportation. Kuwata et al. measured $^{15}\text{N}/^1\text{H}$ HSQC spectra of ^{15}N -labeled β -lactoglobulin as a function of pressure (**Fig. 6**). At 3 MPa, the well-dispersed cross peaks show the fully folded protein structure. Greater than 100 MPa, intensities of these cross peaks decrease and are replaced by a cluster of cross peaks in the central region of the spectra (the random-coil positions), showing an increasing degree of unfolding of the protein structure. The spectral changes were fully reversible with pressure. By examining cross peak intensities of $^{15}\text{N}/^1\text{H}$ HSQC spectra of ^{15}N -labeled β -lactoglobulin as a function of pressure, ΔG^0 and ΔV^0 values were determined for individual amino acid sites according to **Eq. 1** (**Fig. 7**) (**42**). The ΔG^0 values vary considerably from site to site, the noncore side of the barrel (βB , βC , βD , and βE) being comparatively less stable ($\Delta G^0 = 4.6 \pm 1.3$ kcal/mol) than the hydrophobic core side ($\Delta G^0 = 6.5 \pm 2.1$ kcal/mol).

The ΔG^0 values are compared with the free energy differences between the “closed” and “open” conformers independently obtained from hydrogen exchange experiments under the assumption of an EX_2 mechanism (**42**). The

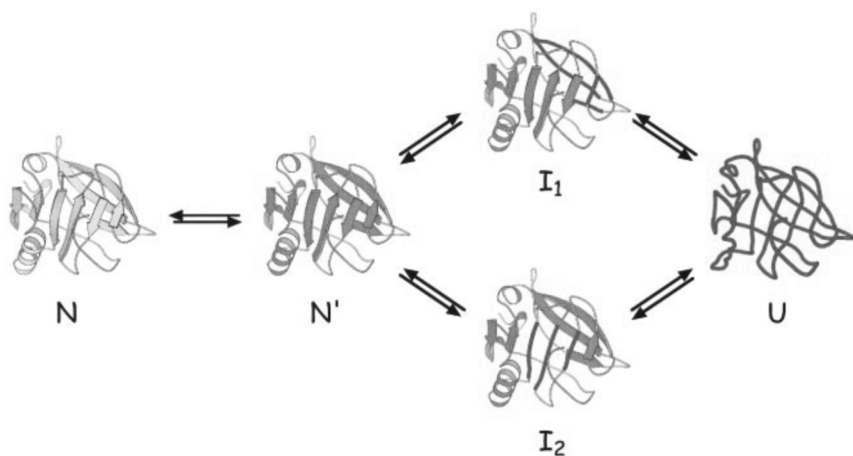


Fig. 8. The conformational equilibrium of β -lactoglobulin revealed by high-pressure NMR. (Reprinted from **ref. 42** with permission from Elsevier.)

good coincidence of ΔG values from high-pressure NMR (**Fig. 6A**) and hydrogen exchange (**Fig. 6B**) in **Fig. 6** indicates that high-pressure NMR is indeed useful to predict conformational fluctuations of a protein in a site-specific manner similarly to a hydrogen exchange experiment. However, the real merit of high-pressure NMR is that it gives not only the information for fluctuation, but also the information on individual structures of the “open” conformers.

The volume change also varies from site to site, the noncore side having a smaller volume change ($\Delta V^\circ = -57.4 \pm 14.4$ mL/mol) than the core side ($\Delta V^\circ = -90.0 \pm 35.2$ mL/mol). This gives an approximate picture of conformational fluctuation such that the noncore side of the barrel fluctuates to produce a group of intermediates I_1 , whereas the hydrophobic core side of the barrel fluctuates to produce a group of intermediates I_2 , which is schematically shown in **Fig. 8**. In the kinetic folding experiments at 1 bar using pulse-labeling $^1\text{H}/^2\text{H}$ NMR techniques (**43**), a kinetic intermediate analogous to the pressure-stabilized equilibrium intermediate I_1 has been observed. Thus the equilibrium scheme shown in **Fig. 8** is likely to also represent the kinetic pathway of folding for β -lactoglobulin (**42**).

Close identity of pressure-stabilized equilibrium intermediates with kinetic intermediates has also been observed for ubiquitin. Kitahara et al. (**27**) performed $^{15}\text{N}/^1\text{H}$ HSQC pressure unfolding measurements at 0°C on ^{15}N -uniformly labeled ubiquitin. The segment between residues 33 and 42 showed lower stability ($\Delta G^0 = 15.2 \pm 1.0$ kJ/mol, $\Delta V^\circ = -58 \pm 4$ mL/mol) than the rest of the protein ($\Delta G^0 = 31.3 \pm 4.7$ kJ/mol, $\Delta V^\circ = -85 \pm 7$ mL/mol), showing that the segment (residues 33–42) preferentially melts to produce an intermediate conformer I.

Kinetic intermediates for ubiquitin were detected by utilizing pulse-labeling $^1\text{H}/^2\text{H}$ NMR techniques combined with GdnHCl-induced refolding (44). Parallel folding pathways were also suggested for this case, the major pathway occurring rapidly with a time constant of 10 ms, the other occurring slowly with a time constant of approx 10 s. In the latter case, the authors suggested an intermediate with Pro-37 and/or Pro 38 in a *cis* conformer is formed, which slowly (~ 10 s) converts into a *trans* conformer. The structure of conformer I is closely identical to that predicted for the slow folding intermediate (~ 10 s) in the kinetic folding experiment (44). The close identity between the pressure-stabilized equilibrium intermediate with the kinetic intermediate is considered to be general rather than exceptional (27).

3.2.5. Experiment 4: Pressure-Jump 1D and 2D NMR

Pressure-jump NMR measurements can be performed for slow folding proteins using the high-pressure NMR system primarily designed for equilibrium studies. This is because very often the folding or unfolding rate becomes extremely slow under pressure. In the case of P13^{MCTP1} (14), just manually changing pressure within minutes is sufficient to observe pressure-jump kinetics intermediates in 1D or even in 2D NMR spectroscopy. For P13^{MCTP1}, it was shown from pressure-jump 2D $^{15}\text{N}/^1\text{H}$ HSQC measurements that the pressure-stabilized intermediate N_2 is closely related to the folding intermediate N_2 revealed by pressure jump to 300 MPa (14). The authors concluded that prior to global unfolding the native structure of P13^{MCTP1} converts into a partially hydrated conformer N_2 , which is still part of the folded ensemble.

Pressure-jump NMR measurements were recently performed on amyloid protofibrils, in which a slow dissociation of the fibrils into monomeric species and reassociation into fibrils were observed upon pressure-jump from 3 to 200 MPa (45). The work symbolizes the utility of pressure in highly associating systems, which may be considered to be an extension of folding.

One of the merits of performing a pressure-jump experiment is that, when carried out as a function of pressure, it can give the activation volume for the reaction, crucial information concerning the structure of the transition state.

3.2.6. Experiment 5: Pressure-Dependent NOESY Experiment: Expressing Folding Intermediates in Atomic Coordinates

Recently, the technology of high-pressure NMR to gain structural information of an intermediate conformer has come to still a higher level of attainment. Kitahara et al. succeeded in obtaining a sufficient numbers of NOESY-based distance constraints along with torsion angle constraints to express the time-averaged structure of ubiquitin at 300 MPa, as well as that at 3 MPa in atomic

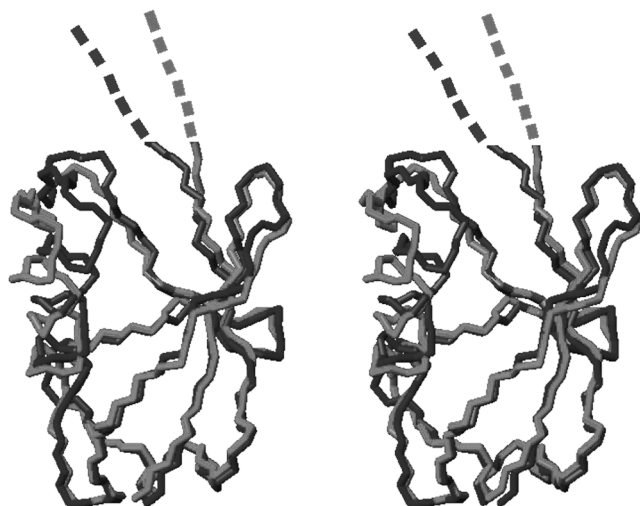


Fig. 9. Stereoview of the superposition of the two ubiquitin structures at 30 bar (black) and 3 kbar (gray) between which the protein fluctuates. (Reprinted from **ref. 46**, with permission from Elsevier.)

coordinates using the program CYANA (46). The two structures of ubiquitin determined at 20°C at 3 and 300 MPa (**Fig. 9**) show globally similar folded structures, but large differences are found in average coordinates, particularly in the C-terminal segment 70–76 and in the helix. At least 3 Å differences are found in C_{α} atoms of the C-terminal side of the helix between the two structures, predicting large amplitude fluctuation of the molecule close to the C-terminal segment carrying the reactive site at its end. From the independent shift analysis, the two structures are considered to closely represent the two extreme structures (N_1 and N_2) between which the protein fluctuates at ambient pressure. The result of this fluctuation is a production of an “open” form of ubiquitin near its C-terminal end, whereas N_2 is considered suitable for interaction with enzymes covalently linking ubiquitin with a substrate protein. Conformer N_2 is too close to N_1 to be considered as a folding intermediate, careful analysis of ^{15}N longitudinal and transverse relaxation rates along with nuclear Overhauser effect gives the lifetime of N_2 to be on the order of 10 μs and only 1.2 kcal/mol energetically higher than N_1 at ambient pressure, thus, it is part of the native ensemble. So far, structure analysis by X-ray or by conventional NMR revealed only conformer N_1 but not the structure of N_2 . But the method shown here can be extended to any intermediate conformers having partially folded segments for which distance constraints may be obtained from NOESY and J-couplings to determine time-averaged atomic coordinates. It is

one of the highlights of high-pressure NMR that it can experimentally determine atomic coordinates of folding intermediates and reveal the biologic important structure.

4. Conclusion

The high-pressure NMR method has a great future for protein folding study. In applying it, one must keep in mind the following:

1. Among the two basic techniques of high-pressure NMR, the on-line cell technique is the method of choice for protein folding study. However, the technique is still in its infancy. More versatile cells must be developed before it is used widely.
2. There are basically two categories of use of high-pressure NMR to protein folding studies. One is the determination of thermodynamic stability (namely ΔG^0) of folded conformer over unfolding along with ΔV^0 . For two-state transitions, this work can be best studied with 1D ^1H NMR. The method may be considered to be alternative to the guanidium chloride or urea denaturation techniques to determine the thermodynamic stability.
3. The second category of the use of high-pressure NMR is to obtain structural information about folding intermediates. This is quite difficult to perform with ^1H NMR. Usually, heteronuclear 2D or multidimensional NMR spectroscopy is to be used.
4. Information on the rate of conformational transition or folding can be obtained using NMR relaxation methods at different pressures or directly by using pressure-jump.

Acknowledgments

This chapter is primarily based on collaborative research. We thank the collaborators, especially Yamada, Sarai, Kuwata, Royer, Kitahara, and Yokoyama. Financial supports from the Ministry of Education, Sports, Culture, Science, and Technology (to K.A.) and from Japan Society for the Promotion of Science (to M. W. L. and K. A.) are gratefully acknowledged.

References

1. Fujisawa, T., Kato, M., and Inoko, Y. (1999) Structural characterization of lactate dehydrogenase dissociation under high pressure studied by synchrotron high pressure small-angle x-ray scattering. *Biochemistry* **38**, 6411–6418.
2. Winter, R. (2002) Synchrotron X-ray and neutron small-angle scattering of lyotropic lipid mesophases, model biomembranes and proteins in solution at high pressure. *Biochim. Biophys. Acta* **1595**, 160–184.
3. Ruan, K. and Balny, C. (2002) High pressure static fluorescence to study macromolecular structure-function. *Biochim. Biophys. Acta* **1595**, 94–102.
4. Ikeuchi, Y., Suzuki, A., Oota, T., et al. (2002) Fluorescence study of the high pressure-induced denaturation of skeletal muscle actin. *Eur. J. Biochem.* **269**, 364–371.

5. Di Venere, A., Salucci, M. L., van Zadelhoff, G., et al. (2003) Structure-to-function relationship of mini-lipoxygenase, a 60-kda fragment of soybean lipoxygenase-1 with lower stability but higher enzymatic activity. *J. Biol. Chem.* **278**, 18,281–18,288.
6. Herberhold, H., Marchal, S., Lange, R., Scheying, C., Vogel, R. F., and Winter, R. (2003) Characterization of the pressure-induced intermediated and unfolded state of red-shifted green fluorescent protein-a static and kinetic FTIR, UV-VIS and fluorescence spectroscopy study. *J. Mol. Biol.* **330**, 1153–1164.
7. Dzwolak, W., Kato, M., and Taniguchi, Y. (2002) Fourier-transform infrared spectroscopy in high pressure studies on proteins. *Biochim. Biophys. Acta* **1595**, 131–144.
8. Smeller, L., Meersmann, F., Fidy, J., and Heremans, K. (2003) High pressure FTIR study of the stability of horseradish peroxidase. Effect of heme substitution, ligand binding, Ca⁺⁺ removal, and reduction of the disulfide bonds. *Biochemistry* **42**, 553–561.
9. Meersman, F., Smeller, L., and Heremans, K. (2002) Comparative fourier transform infrared spectroscopy study of cold-, pressure-, and heat-induced unfolding and aggregation of myoglobin. *Biophys. J.* **82**, 2635–2644.
10. Jung, C., Kozin, S. A., Canny, B., Chervin, J. C., and Hoa, G. H. (2003) Compressibility and uncoupling of cytochrome P450cam: high pressure FTIR and activity studies. *Biochem. Biophys. Res. Commun.* **312**, 197–203.
11. Lange, R. and Balny, C. (2002) UV-visible derivative spectroscopy under high pressure. *Biochim. Biophys. Acta* **1595**, 80–93.
12. Pappenberger, G., Saudan, C., Becker, M., Merbach, A. E., and Kiefhaber, T. (2000) Denaturant-induced movement of the transition state of protein folding revealed by high-pressure stopped-flow measurements. *Proc. Natl. Acad. Sci. USA* **97**, 17–22.
13. Jung, C., Bec, N., and Lange, R. (2002) Substrates modulate the rate-determining step for CO binding in cytochrome P450cam (CYP101). *Eur. J. Biochem.* **269**, 2989–2996.
14. Kitahara, R., Royer, C., Yamada, H., et al. (2002) Equilibrium and pressure-jump relaxation studies of the conformational transitions of P13MTCP1. *J. Mol. Biol.* **320**, 609–628.
15. Desai, G., Panick, G., Zein, M., Winter, R., and Royer, C. A. (1999) Pressure-jump studies of the folding/unfolding of trp repressor. *J. Mol. Biol.* **288**, 461–475.
16. Woenckhaus, J., Koehling, R., Thiagarajan, P., et al. (2001) Pressure-jump small-angle x-ray scattering detected kinetics of staphylococcal nuclease folding. *Biophys. J.* **80**, 1518–1523.
17. Kitamura, Y. and Itoh, T. (1987) Reaction volume of protonic ionization for buffering agents. Prediction of pressure dependence of pH and pOH. *J. Solution Chemistry* **16**, 715–725.
18. Jonas, J. (2002) High-resolution nuclear magnetic resonance studies of proteins. *Biochim. Biophys. Acta* **1595**, 145–159.

19. Akasaka, K. and Yamada, H. (2001) On-line cell high-pressure nuclear magnetic resonance technique: application to protein studies. *Methods Enzymol.* **338**, 134–158.
20. Arnold, M. R., Kalbitzer, H. R., and Kremer, W. (2003) High-sensitivity sapphire cells for high pressure NMR spectroscopy on proteins. *J. Magnetic Resonance* **161**, 127–131.
21. Urbauer, J. L., Ehrhardt, M. R., Bieber, R. J., Flynn, P. F., and Wand, J. A. (1996) High-resolution triple-resonance NMR spectroscopy of a novel calmodulin peptide complex at kilobar pressures. *J. Am. Chem. Soc.* **118**, 11,329–11,330.
22. Royer, C. A., Hinck, A. P., Loh, S. N., et al. (1993) Effects of amino acid substitutions on the pressure denaturation of *staphylococcal* nuclease as monitored by fluorescence and nuclear magnetic resonance spectroscopy. *Biochemistry* **32**, 5222–5232.
23. Yamada, H., Nishikawa, M., Honda, M., Shimura, T., Akasaka, K., and Tabayashi, K. (2001) Pressure-resisting cell for high-pressure, high-resolution nuclear magnetic resonance measurements at very high magnetic fields. *Rev. Sci. Instrum.* **72**, 1463–1471.
24. Kamatari, Y. O., Kitahara, R., Yamada, H., Yokoyama, S., and Akasaka, K. (2004) High-pressure NMR spectroscopy for characterizing folding intermediates and denatured states of proteins. *Methods* **34**, 133–143.
25. Kuwata, K., Kamatari, Y. O., Akasaka, K., and James, T. L. (2004) Slow conformational dynamics in the hamster prion protein. *Biochemistry* **43**, 4439–4446.
26. Kuwata, K., Li, H., Yamada, H., and Legname, G. (2002) Locally disordered conformer of the hamster prion protein: a crucial intermediate to PrP^{Sc}? *Biochemistry* **41**, 12,277–12,283.
27. Kitahara, R. and Akasaka, K. (2003) Close identity of a pressure-stabilized intermediate with a kinetic intermediate in protein folding. *Proc. Natl. Acad. Sci. USA* **100**, 3167–3172.
28. Lassalle, M. W., Yamada, H., Morii, H., Ogata, K., Sarai, A., and Akasaka, K. (2001) Filling a cavity dramatically increases pressure stability of the c-myc R2 subdomain. *Proteins* **45**, 96–101.
29. Lassalle, M. W., Yamada, H., and Akasaka, K. (2000) The pressure-temperature free energy-landscape of *staphylococcal* nuclease monitored by ¹H NMR. *J. Mol. Biol.* **298**, 293–302.
30. Niraula, T. N., Konno, T., Li, H., Yamada, H., Akasaka, K., and Tachibana, H. (2004) Pressure-dissociable reversible assembly of intrinsically denatured lysozyme is a precursor for amyloid fibrils. *Proc. Natl. Acad. Sci. USA* **101**, 4089–4093.
31. Akasaka, K. (2003) Highly fluctuating protein structure revealed by variable-pressure nuclear magnetic resonance. *Biochemistry* **42**, 10,875–10,885.
32. Chan, H. S. and Dill, K. A. (1998) Protein folding in the landscape perspective: Chevron plots and non-Arrhenius kinetics. *Proteins* **30**, 2–33.
33. Smeller, L. and Heremans, K. (1997) Some thermodynamic and kinetic consequences of the phase diagram of protein denaturation. In: *High-Pressure Research in the Biosciences and Biotechnology* (Heremans, K., ed.), Leuven University Press, Leuven, Belgium, pp. 55–58.

34. Panick, G., Vidugiris, G. J. A., Malessa, R., Rapp, G., Winter, R., and Royer, C. A. (1999) Exploring the temperature-pressure phase diagram of *staphylococcal* nuclease. *Biochemistry* **38**, 4157–4164.
35. Panick, G., Malessa, R., Winter, R., Rapp, G., Frye, K. J., and Royer, C. A. (1998) Structural characterization of the pressure-denatured state and unfolding/refolding kinetics of *staphylococcal* nuclease by synchrotron small-angle x-ray scattering and fourier-transform infrared spectroscopy. *J. Mol. Biol.* **275**, 389–402.
36. Akasaka, K. (2003) Exploring the entire conformational space of proteins by high-pressure NMR. *Pure. Appl. Chem.* **75**, 927–936.
37. Chalikian, T. V. (2003) Volumetric properties of proteins. *Annu. Rev. Biophys. Biomol. Struct.* **32**, 207–235.
38. Frye, K. and Royer, C. A. (1998) Probing the contribution of internal cavities to the volume change of protein unfolding under pressure. *Protein Sci.* **7**, 2217–2222.
39. Imai, T., Harano, Y., Kovalenko, A., and Hirata, F. (2001) Theoretical study for volume changes associated with the helix-coil transition of peptides. *Biopolymers* **59**, 512–519.
40. Royer, C. (2002) Revisiting volume changes in pressure induced proteins unfolding. *Biochim. Biophys. Acta* **1595**, 201–209.
41. Ogata, K., Kanei-Ishii, C., Sasaki, M., et al. (1996) The cavity in the hydrophobic core of Myb-DNA-binding domain is reserved for DNA recognition and trans-activation. *Nat. Struct. Biol.* **3**, 178–187.
42. Kuwata, K., Li, H., Yamada, H., Batt, C.A., Goto, Y., and Akasaka, K. (2001) High pressure NMR reveals a variety of fluctuating conformers in β -lactoglobulin. *J. Mol. Biol.* **305**, 1073–1083.
43. Forge, V., Hoshino, M., Kuwata, K., et al. (2000) Is folding of β -lactoglobulin non-hierarchic? Intermediate with native-like β -sheet and non-native α -helix. *J. Mol. Biol.* **296**, 1039–1051.
44. Briggs, M. S. and Roder, H. (1992) Early hydrogen-bonding events in the folding reaction of ubiquitin. *Proc. Natl. Acad. Sci. USA* **89**, 2017–2021.
45. Kamatari, Y. O., Yokoyama, S., Tachibana, H., and Akasaka, K. (2005) Pressure-jump NMR study of dissociation and association of amyloid protofibrils, *J. Mol. Biol.* **349**, 916–921.
46. Kitahara, R., Yokoyama, S., and Akasaka, K. (2005) NMR snapshots of a fluctuating protein structure: Ubiquitin at 30 bar – 3kbar. *J. Mol. Biol.* **347**, 277–285.



<http://www.springer.com/978-1-58829-622-1>

Protein Folding Protocols

Bai, Y. (Ed.)

2006, XIV, 328 p. 111 illus., Hardcover

ISBN: 978-1-58829-622-1

A product of Humana Press